Redox Biology 15 (2018) 1–11

Contents lists available at ScienceDirect

Redox Biology

journal homepage: www.elsevier.com/locate/redox

Research paper

Oxidized LDL triggers changes in oxidative stress and inflammatory biomarkers in human macrophages

Oscar J. Lara-Guzmán[a], Ángel Gil-Izquierdo[b], Sonia Medina[b], Edison Osorio[c], Rafael Álvarez-Quintero[c], Natalia Zuluaga[a], Camille Oger[d], Jean-Marie Galano[d], Thierry Durand[d], Katalina Muñoz-Durango[a,*]

[a] Vidarium, Nutrition, Health and Wellness Research Center, Nutresa Business Group. Calle 8 Sur No. 50-67, Medellín, Colombia
[b] Research Group on Quality, Safety and Bioactivity of Plant Foods, Department of Food Science and Technology, CEBAS (CSIC), P.O. Box 164, 30100 Campus University Espinardo, Murcia, Spain
[c] Grupo de Investigación en Sustancias Bioactivas, Facultad de Ciencias Farmacéuticas y Alimentarias, Universidad de Antioquia, Calle 70 No. 52-21, Medellín, Colombia
[d] Institut des Biomolécules Max Mousseron (IBMM), UMR 5247, CNRS, University of Montpellier, ENSCM, Faculty of Pharmacy, Montpellier, France

ARTICLE INFO

Keywords:
Macrophages
OxLDL
Oxylipins
Isoprostanes
Prostaglandins
Foam cells

ABSTRACT

Oxidized low-density lipoprotein (oxLDL) is a well-recognized proatherogenic particle that functions in atherosclerosis. In this study, we established conditions to generate human oxLDL, characterized according to the grade of lipid and protein oxidation, particle size and oxylipin content. The induction effect of the cellular proatherogenic response was assessed in foam cells by using an oxLDL-macrophage interaction model. Uptake of oxLDL, reactive oxygen species production and expression of oxLDL receptors (CD36, SR-A and LOX-1) were significantly increased in THP-1 macrophages. Analyses of 35 oxylipins revealed that isoprostanes (IsoP) and prostaglandins (PGs) derived from the oxidation of arachidonic, dihomo gamma-linolenic and eicosapentaenoic acids were strongly and significantly induced in macrophages stimulated with oxLDL. Importantly, the main metabolites responsible for the THP1-macrophage response to oxLDL exposure were the oxidative stress markers 5-*epi*-5-F_{2t}-IsoP, 15-E_{1t}-IsoP, 8-F_{3t}-IsoP and 15-keto-15-F_{2t}-IsoP as well as inflammatory markers PGDM, 17-*trans*-$PGF_{3\alpha}$, and 11β-$PGF_{2\alpha}$, all of which are reported here, for the first time, to function in the interaction of oxLDL with THP-1 macrophages. By contrast, a salvage pathway mediated by anti-inflammatory PGs (PGE_1 and 17-*trans*-$PGF_{3\alpha}$) was also identified, suggesting a response to oxLDL-induced injury. In conclusion, when THP-1 macrophages were treated with oxLDL, a specific induction of biomarkers related to oxidative stress and inflammation was triggered. This work contributes to our understanding of initial atherogenic events mediated by oxLDL-macrophage interactions and helps to generate new approaches for their modulation.

1. Introduction

Macrophage foam cells play an important role in atherosclerosis development. They induce reactive oxygen species (ROS) production, inflammatory responses and accumulation of lipids, which lead to fatty streak formation in the vascular wall [1]. Hypercholesterolemia is directly linked to key events in plaque progression, during which oxidative stress (OS) and inflammation are relevant [2]. An increase in circulating oxLDL is considered to be a primary contributor to the induction of foam cells in the arterial intima, where massive uptake of oxLDL by macrophages occurs via scavenger receptors (i.e., SR-A and CD36) and lectin-like oxLDL receptor-1 (LOX-1) [3,4]. OxLDL also activates SR/Toll-like receptor cooperative signaling pathways in macrophages, leading to the induction of pro-inflammatory downstream signaling cascades, ROS production and IL-1β maturation via NLRP3 inflammasomes [5,6]. In atherosclerosis-related inflammation,

Abbreviations used: AA, arachidonic acid; AAPH, 2,2′-Azobis (2-methylpropionamidine) dihydrochloride; BHT, butylated hydroxytoluene; BMI, body mass index; CVD, cardiovascular diseases; C-SMP, cell-surface marker proteins; DGLA, Dihomo-gamma-linolenic acid; DLS, dynamic light scattering; ETDA, ethylenediaminetetraacetic acid; EPA, eicosapentaenoic acid; ESI, electrospray ionization; FRAP, ferric reducing antioxidant power assay; IsoP, isoprostane; LDL, low-density lipoprotein; LDH, lactate dehydrogenase; LC, liquid chromatography; oxLDL, oxidized low-density lipoprotein; MDA, malondialdehyde; MFI, mean fluorescence intensity; MRM, multiple reaction monitoring; MS, mass spectrometry; OS, oxidative stress; PBS, phosphate-buffered saline; PMA, phorbol 12-myristate-13-acetate; PGs, Prostaglandins; PUFA, polyunsaturated fatty acids; REM, relative electrophoretic mobility; ROS, reactive oxygen species; SPE, solid phase extraction; SR, scavenger receptor; TBARS, thiobarbituric acid-reactive substances; TLR, toll-like receptor; Trolox, (±) − 6-Hydroxy-2,5,7,8-tetramethylchromane-2-carboxylic acid; TX, thromboxane; UHPLC, ultra-high performance liquid chromatography

* Corresponding author.
E-mail address: kmunoz@serviciosnutresa.com (K. Muñoz-Durango).

https://doi.org/10.1016/j.redox.2017.11.017
Received 27 September 2017; Received in revised form 1 November 2017; Accepted 18 November 2017
Available online 22 November 2017

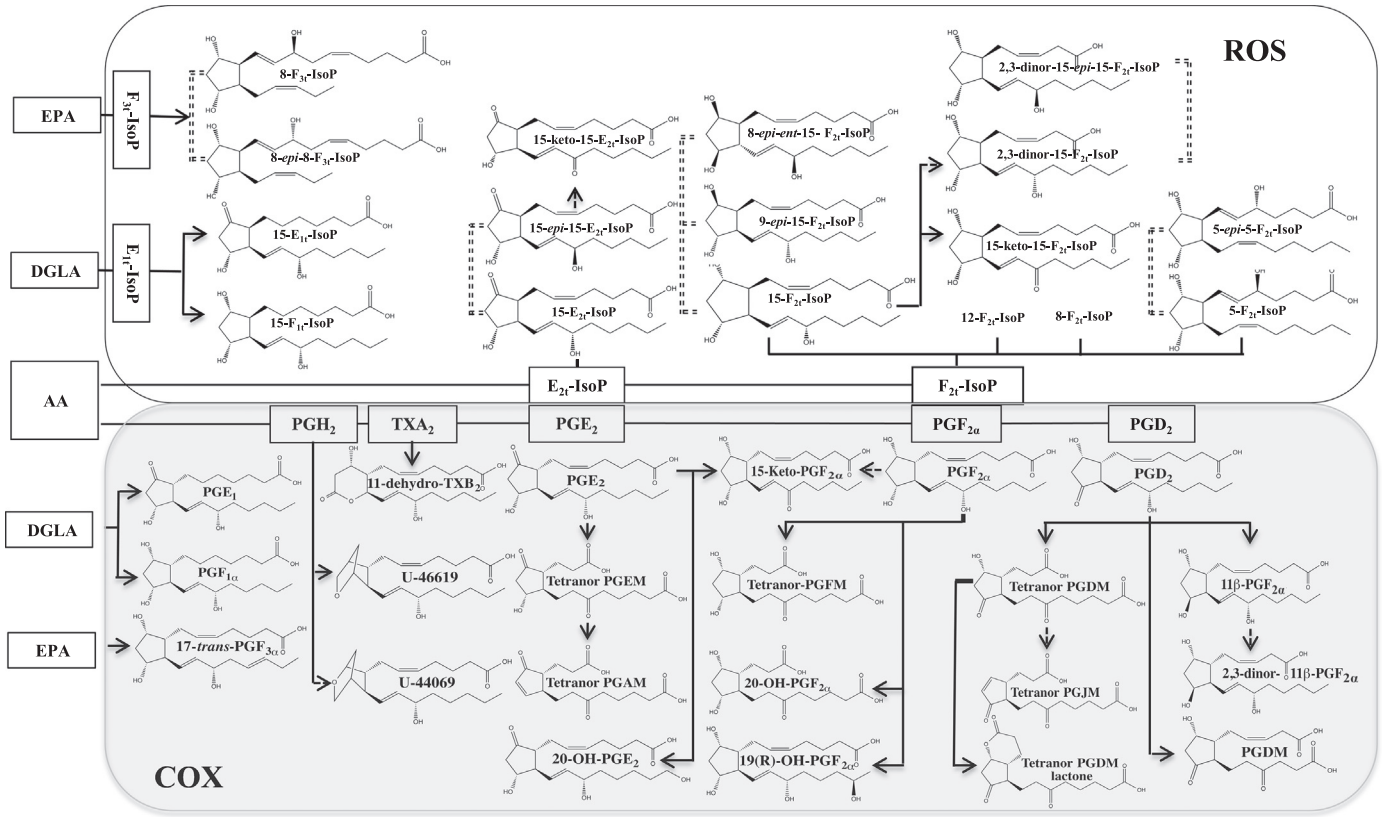

Scheme 1. Oxylipins derived from arachidonic acid C20:4 (AA), dihomo-gamma-linolenic acid C20:3 (DGLA) (omega-6 fatty acids) and eicosapentaenoic acid C20:5 (EPA) (omega-3 fatty acid). In gray: via cyclooxygenase (COX); in white: via reactive oxygen species (ROS). (= =) stereoisomers.

macrophages are regulated by numerous cytokines and chemokines, and the balance between pro- and anti-inflammatory signals determines plaque stability [1,5].

In the complex inflammatory context of atherosclerosis, macrophages also produce several lipid mediators known as oxylipins (isoprostanes and prostaglandins), which usually have negative effects [7]. Isoprostanes (IsoPs) are prostaglandin-like compounds that are produced *in vivo* by free radical-induced peroxidation of arachidonic acid (AA) [8]. They are generally considered to be OS markers and potentially mediate several of the adverse effects associated with oxidant injury [8]. These compounds are produced *in situ* in membrane phospholipids and are then released in their free form into circulation [9]. Prostaglandins (PGs), by contrast, are bioactive signaling molecules derived from cyclooxygenase (COX) and subsequent PG synthase activity on AA [7]. Several oxylipins are recognized as biomarkers of acute or chronic inflammation and are related to several pathologies, such as atherosclerosis, diabetes, ischemia-reperfusion, hypertension and obesity, as well as smoking [7,10,11]. Therefore, assessment of PGs and IsoPs in biological samples offers an opportunity to understand lipid metabolism, determine potential targets and characterize the relationship between oxidative stress and inflammation in atherogenesis [12,13].

In macrophage foam cells, a full physicochemical characterization of oxLDL is fundamental to understanding the biology of the cell. OxLDL may exist in multiple forms with different degrees of oxidation under physiological and *in vitro* conditions [14]. However, the previous differences in results obtained using this model can be primarily attributed to the heterogeneity in oxLDL preparation. Therefore, it is imperative to standardize conditions, such as the oxidants used, time, exposure, concentration and LDL source, for oxLDL generation and subsequent characterization [14]. Lipid and protein LDL modifications can be monitored by thiobarbituric acid-reactive substances (TBARS), relative electrophoretic mobility (REM) and particle size, which provide information concerning the features of oxLDL [15–17]. Related to oxylipin determination, the most suitable technique for simultaneous assessment of PGs and IsoPs in biological samples is UPLC/MS/MS [18]; through targeted lipidomics, hundreds of lipids in foam cells have been determined [18,19]. This analytical strategy has expanded the understanding of the effects of lipid mediators in the regulation of diverse cellular processes [20], as well as the role of oxylipins in macrophages and foam cells during the atherogenic process [19,21].

Despite the extensive literature concerning oxLDL-macrophage interactions and foam cell formation, both the induction effect of oxLDL on oxylipin production in macrophages as well as its association with biomarkers related to atherosclerotic lesions are poorly understood. To investigate the relationship between OS, inflammation and foam cell formation, we utilized a targeted lipidomic approach to perform functional analyses on THP-1 macrophages treated with human oxLDL. The aim of this study was to generate oxLDL under controlled conditions and to fully characterize and assess its effects on THP-1 macrophage oxylipin profiles. A total of 35 oxylipins related to inflammation and OS were screened by UHPLC–QqQ–MS/MS [22]. Remarkably, we report for the first time the induction of 8 PGs and 8 IsoPs as a result of oxLDL-THP-1 macrophage interactions, two of which have anti-inflammatory activity.

2. Material and methods

2.1. Chemicals and reagents

All LC–MS grade solvents, sodium acetate, trichloroacetic acid and $FeCl_3$ were obtained from J.T. Baker (Phillipsburg, New Jersey, USA). Formic acid was purchased from Panreac (Castellar Del Vallés, Barcelona, Spain). 2,4,6-Tris (2-pyridyl)-s-triazine (TPTZ), 2,2′-azobis (2-methylpropionamidine) dihydrochloride (AAPH), (±)−6-hydroxy-2,5,7,8-tetramethylchromane-2-carboxylicacid (Trolox), 2-

thiobarbituric acid (TBA), 1,1,3,3-tetramethoxypropane (malondialdehyde (MDA) standard), 37% HCl, BIS–TRIS (Bis-(2-hydroxyethyl)-amino-tris(hydroxymethyl)-methane), zinc sulfate and β-glucuronidase from *Helix pomatia* (type H-2) were obtained from Sigma–Aldrich (St. Louis, Missouri, USA). The solid phase extraction (SPE) cartridges (Strata X and X-AW, 100 mg, 3 mL^{-1}) were from Phenomenex (Torrance, California, USA).

Thirty-five oxylipins (Scheme 1), including seven isoprostanes (15-F_{2t}-IsoP; 15-keto-15-F_{2t}-IsoP; $PGF_{2\alpha}$; 9-*epi*-15-F_{2t}-IsoP; 15-keto-15-E_{2t}-IsoP; 15-E_{1t}-IsoP; 15-F_{1t}-IsoP), twenty prostaglandins (PGE_2; tetranor-PGEM (tetranor-PGE-metabolite); tetranor-PGAM (tetranor-PGA-metabolite); 20-OH-PGE_2; 15-keto $PGF_{2\alpha}$; tetranor PGFM (tetranor-PGF-metabolite); 20-OH-$PGF_{2\alpha}$; 19(R)-OH-$PGF_{2\alpha}$; PGD_2; 11β-$PGF_{2\alpha}$; 2,3-dinor-11β-$PGF_{2\alpha}$; PGDM (PGD-metabolite); tetranor-PGDM (tetranor-PGD-metabolite); tetranor-PGJM (tetranor-PGJ-metabolite); tetranor-PGJM lactone; 9,11-dideoxy-9α,11α-methanoepoxy $PGF_{2\alpha}$ (U-46619); 9,11-dideoxy-9α,11α-epoxymethano $PGF_{2\alpha}$ (U-44069); PGE_1; $PGF_{1\alpha}$; and 17-*trans*-$PGF_{3\alpha}$) and one thromboxane (11-dehydro thromboxane B_2 (TXB_2)) were from Cayman Chemicals (Ann Arbor, Michigan, USA). Seven additional isoprostanes (2,3-dinor-15-F_{2t}-IsoP; 2,3-dinor-15-*epi*-15-F_{2t}-IsoP; 5-F_{2t}-IsoP; 5-*epi*-F_{2t}-IsoP; 15-*epi*-15-E_{2t}-IsoP; 8-F_{3t}-IsoP and 8-*epi*-8-F_{3t}-IsoP) were synthesized by Durand´s Team at the Institut des Biomolécules Max Mousseron (IBMM), (Montpellier, France) according to previous published procedures [23–27].

2.2. LDL sample

The LDL were obtained from 15 volunteers (6 men and 9 women) aged between 19 and 30 years old with body mass indexes (BMI) between 19.0 and 27.9 kg/m^2, who participated in a clinical trial approved by the CES University Ethics Committee (Act 47; 50 project code 142; registered at registroclinico.sld.cu as RPCEC00000168). Specific characteristics of volunteers were described in a previous report [28]. The blood samples were collected in EDTA (1 mg mL^{-1}) and centrifuged at 600*xg* for 15 min at 4 °C. All plasma samples were mixed and stored at −80 °C until use. An aliquot of plasma from each subject was reserved for biochemical analysis.

2.3. Biochemical analysis

The concentration of oxLDL was measured by ELISA (Mercodia kit; Uppsala, Sweden). The antioxidant capacity of the plasma was determined by ferric reducing antioxidant power assay (FRAP), according to Lara-Guzmán et al. [29]. The FRAP reaction was monitored in a microwell plate assay, and the Trolox calibration solutions (31.25–1000 mM) were prepared in PBS. The results are expressed as μmol TE L^{-1} of plasma. The ELISA and FRAP measurements were performed at 450 nm and 593 nm, respectively, using a Synergy HT Multi-Mode Microplate Reader (BioTek Instruments, Inc., Winooski, USA).

2.4. LDL isolation

LDL was purified from pooled plasma via discontinuous density gradient centrifugation using a Beckman XL-100 ultracentrifuge (Brea, CA, USA) according to Jiménez et al., with minor modifications [30]. The LDL fraction was collected and desalted by ultrafiltration with Amicon® Ultra 0.5 mL, Ultracel 3 K (Tullagreen, Cork, IRL) against five-fold PBS at 16,000 × *g* for 10 min at 4 °C. The concentrated LDL was diluted in PBS, filtered (0.22 μm, sterile) and stored at 4 °C until use. The purification of the LDL fraction was confirmed by SDS/PAGE, and the protein concentration was measured by a commercial kit using bicinchoninic acid (Pierce BCA Protein Assay Kit; Rockford, Illinois, USA).

2.5. LDL oxidation and physicochemical characterization

2.5.1. Oxidation

Two different oxidants were used to establish the optimal conditions for LDL oxidation. LDL at 500 μg mL^{-1} was incubated between 3 and 18 h at 37 °C with two different oxidants: $CuSO_4$ at 1.0, 5.0 and 10 μM, and AAPH at 1.0, 5.0 and 10 mM. The oxidation was stopped by the addition of 1% EDTA. The extent of lipid peroxidation was determined by the TBARS method, and the values are expressed as nM of MDA [30].

2.5.2. Relative electrophoretic mobility (REM)

The changes in the net charge of the LDL protein fraction (Apo B 100) were determined by REM according to Vieira et al., with minor modifications [31]. The electrophoresis was carried out using agarose gel (0.8%), performed at 120 V and 500 mA in 0.05 M barbital buffer (pH 8.6) for 1 h. The bands were fixed for 30 min in a solution containing ethanol: glacial acetic acid (60:10). The gel was stained with Sudan black B (0.1% *w/v* in 60% ethanol) for lipids or Coomassie blue for proteins (0.125% *w/v* in 60% methanol and 10% glacial acetic acid).

2.5.3. Size of the particles

The size of the LDL and oxLDL particles was determined by dynamic light scattering (DLS) with a Nano-ZS instrument (Malvern, Worcs. UK) equipped with a 4 mW He–Ne laser (633 nm) operating at a 90° angle and 25 °C. The LDL and oxLDL at 100 μg mL^{-1} were diluted in PBS. The experiments were performed in triplicate, and the results were analyzed in Zetasizer software.

2.6. THP-1 macrophage culture and treatments

2.6.1. Culture

THP-1 monocytes (ATCC® TIB-202™) were cultured in RPMI-1640 medium (with GlutaMAX™ and 25 mM Hepes) supplemented with 10% (*v/v*) fetal bovine serum (FBS), 100 μg mL^{-1} penicillin and 100 μg mL^{-1} streptomycin. The cell culture was maintained in a humidified atmosphere containing 5% CO_2 at 37 °C. THP-1 differentiation was induced with 100 nM phorbol 12-myristate-13-acetate (PMA) for 72 h. Non-adherent cells were removed by aspiration of the supernatant followed by two washes with PBS and replacement with fresh medium supplemented without PMA at least 24 h before the experimental procedure. Cells were seeded in 96-well plates (0.5–1.5 × 10^5 cells/well) for colorimetric and spectrofluorometric analysis; 48-well plates (3 × 10^5 cells/well) for flow cytometry analysis; and 24-well plates (1 × 10^6 cells/well) for UHPLC–QqQ–MS/MS analysis. Three treatment groups of macrophages were used: a control group (no treatment) and two treatment groups – one with oxLDL and the other with native LDL. The oxLDL-treated group was cultured in cell media containing three different concentrations of oxLDL (31.25 to 100 μg mL^{-1}). The length of exposure to oxLDL depended on the assay as follows: (a) 36 h for cell viability and oxLDL membrane receptor experiments; (b) 6 h for the uptake of DiI-oxLDL experiments; (c) 1 h for ROS production experiments; and (d) 1, 6 and 12 h for targeted lipidomic analysis. The LDL-treated group was stimulated with 12.5–100 μg mL^{-1} LDL depending on the assay.

2.6.2. Cell viability

To evaluate cell viability, LDH activity was determined in the culture medium collected after the treatment period using a commercial viability test (LDH assay kit; Promega, Madison, WI) at 340 nm using a synergy HT multi-mode microplate reader (BioTek Instruments, Inc.; Winooski, Vermont, USA). The results are expressed as percentage cell viability. Three independent assays were performed in triplicate.

2.6.3. ROS production

The control group was incubated with PBS and the treated groups were incubated for 1 h with 100 μg mL^{-1} of LDL or oxLDL

(6.25–100 μg mL^{-1}). Cells were then simultaneously incubated with 2 μM of the fluorescent ROS-sensitive substrate CM-H_2DCFDA Invitrogen™ (Carlsbad, California, USA) for 1 h at 37 °C, washed twice, re-suspended in PBS, and analyzed by flow cytometry.

2.6.4. OxLDL uptake

To generate DiI-oxLDL, LDL was labeled with the DiI Vybrant® Multicolor Cell-Labeling Kit (Carlsbad, California, USA) as described previously, with slight modifications [32]; 1 mg mL^{-1} of LDL was incubated with 0.1 μg mL^{-1} DiI or DiO for 12 h at 37 °C under a nitrogen atmosphere in the dark. The DiI-LDL complex (0.5 mg mL^{-1}) was then oxidized (Cu_2S0_4 5 μM; 6 h; 37 °C). Unbound dye in DiI-oxLDL or DiO-LDL particles and copper ions from the oxidation step were removed through ultrafiltration with Amicon® as previously described. The uptake of DiI-oxLDL by macrophages was analyzed by flow cytometry. Cells were incubated with DiI-oxLDL at 6.25–25 μg mL^{-1} for 6 h. To test the specificity of uptake, the macrophages were treated with 10 μg mL^{-1} DiI-oxLDL and a 10-fold excess of unlabeled oxLDL for 6 h. After treatments, the cells were washed three times with PBS and harvested with trypsin solution (0.25% trypsin, 0.02% EDTA). Then, the macrophages were centrifuged at 300*xg* for 5 min, washed once with RPMI 1640/10% FBS at 37 °C and twice with PBS at 300*xg* for 5 min at 4 °C.

The expression of oxLDL receptors at the cell surface was evaluated by flow cytometry. CD14, CD36, SR-A and LOX-1 were the cell-surface protein markers analyzed. The macrophage cultures were stimulated with oxLDL (6.25–50 μg mL^{-1}) for 12, 24 and 36 h, washed and harvested with 0.2% EDTA in PBS at 37 °C. Nonspecific binding of antibodies was blocked by incubating cells in 10% FCS-PBS. Cells were incubated with purified human monoclonal antibodies (R&D Systems; Minneapolis, Minnesota, USA), CD36/SR-B3 fluorescein (clone 255606; Cat#FAB19551F, RRID:AB_1026194), SR-A/MSR1 phycoerythrin (clone 361615; Cat#FAB2708P, RRID:AB_2044631), LOX-1/OLR1 PerCP (clone 331212; Cat#FAB1798P, RRID:AB_10718092), CD14 Alexa Fluor (clone 134620; Cat#FAB3832N, RRID:AB_1097193) or the isotype control rat IgG2B fluorescein (clone 141945; Cat# IC013F, RRID:AB_357258), mouse IgG2B phycoerythrin (clone 133303; Cat#IC0041P, RRID:AB_357249, mouse IgG2B PerCP (clone 133303; Cat#IC0041C, RRID:AB_1207938) and mouse IgG1 Alexa Fluor (clone11711; Cat# IC002N, RRID:AB_10972478), using 1 μL per 100,000 cells, and analyzed by flow cytometry.

2.6.5. Flow cytometry analysis

ROS production (DCF), DiI-oxLDL uptake and oxLDL receptors in macrophages were analyzed with a FACS Canto II flow cytometer (Beckton Dickinson; San José, California, USA) for all acquisitions (at least 10,000 events). Analysis was performed with FlowJo software. For the analysis of DiI-oxLDL and ROS, the data were calculated by subtracting the cell auto-fluorescence from the fluorescence of the treated samples and expressed as the mean fluorescence intensity (MFI) and positive cell percentage for DiI+ or DCF+. The oxLDL receptors were reported as the positive cell percentages of CD36+, SR-A+, or LOX-1+ and their respective MFIs.

2.7. Extraction of oxylipins from cells, culture medium, LDL and oxLDL

Oxylipins were assessed in cells and in culture media of THP-1 macrophages stimulated with oxLDL or LDL (12.5, 25 and 50 μg mL^{-1}) at 1, 6 and 12 h, according to a previous report [33]. After the treatments, the culture medium was collected and supplemented with BHT (0.05% *v/v*). The monolayer (1×10^6 cells/well) was incubated with 500 μL of lysis buffer (50 mM Tris-HCl pH 8.0, 150 mM NaCl, 1% Triton X-100, containing 0.005% BHT and EDTA 1 mM) for 1 h at 0 °C and harvested. Culture medium and lysate samples were kept at −80 °C until the oxylipin extraction. To precipitate proteins, 500 μL of culture medium or lysate samples for analysis was mixed with 500 μL zinc sulfate (0.1 M) and spun centrifuged at 10,000 × *g* for 5 min. The supernatants were hydrolyzed using ~5000 UE mL^{-1} of *β*-glucuronidase type H2 from *Helix pomatia* in 0.1 M acetate buffer (pH 4.9) for 2 h at 37 °C. Methanol/HCl 200 mM (500 μL) was added to the mix and centrifuged at 10,000 × *g* for 5 min to precipitate the proteins. Supernatants (1 mL) were mixed with 1250 μL methanol and 2 mL bis-tris buffer 0.02 M HCl (pH 7.0) and subjected to solid-phase extraction (SPE) using a Strata X-AW cartridge (100 mg 3 mL^{-1}). For the extraction of oxylipins from LDL and oxLDL (400 μL at 500 μg mL^{-1}) the same procedure was applied. Target compounds were eluted with 1 mL methanol and dried using a SpeedVac concentrator before injection. The sample volume injected was 20 μL (model Savant, ThermoFisher Scientific, USA) [34]. This method evaluates oxylipins after the phospholipase action (free and glucuronidated) but not those linked to phospholipids [35].

2.8. UHPLC-QqQ-MS/MS analyses

The separation of IsoPs (14), thromboxane (Tx) (1), and PGs (20) in macrophages and supernatants was performed using UHPLC coupled with 6460 QqQ-MS/MS (Agilent Technologies; Waldbronn, Baden-Württemberg, Germany) using the set-up described by Medina et al. [22] with modifications. The chromatographic separation was performed on an Acquity UPLC BEH C18 column (2.1 × 150 mm, 1.7 μm; Waters), the column temperatures were 6 °C. The mobile phases employed were solvent A (H2O/acetic acid; 99.99:0.01, *v/v*) and B (MeOH/acetic acid; 99.99:0.01, *v/v*). The flow rate was 0.15 mL min^{-1} using a linear gradient scheme (minutes; %B): (0.00; 60), (7.00; 60), (7.01; 73), (10.00; 73), (10.01; 80), (18.00; 100), (19.00; 100), and (19.01; 60). The MS analysis was applied in the MRM (multiple reaction monitoring) quantification mode using negative ESI (MS optimized parameters are detailed in Table S1). The internal standards were 11-dehydro TXB_2d_4 (fragmentor: 120; collision energy: 10) and 8-iso-$PGF_{2\alpha}d_4$ (fragmentor: 130; collision energy: 22). The operating conditions for the MS parameters were as follows: gas flow: 8 L min^{-1}, nebulizer: 30 psi, capillary voltage: 4000 V, nozzle voltage: 2750 V, gas temperature: 325 °C and jetstream gas flow: 8 L min^{-1}. The acquisition time was 19.01 min for each sample, with a post-run time of 3.0 min for column equilibration. The MS fragmentor parameters (ion optics; capillary exit voltage) and collision energy of the new analytes were optimized for each compound to generate the most-abundant product ions. The MS parameters ranged from 50 to 160 V and the collision energy ranged from 0 to 24 V. The quantification of IsoPs, PGs, and TX detected was performed using authentic markers (*section 2.1.1c*. The PGs, IsoPs, and TX) calculated from the area ratio of the ion peak of each compound to that of the corresponding standard. Data acquisition and processing were performed using MassHunter software version B.04.00 (Agilent Technologies).

2.9. Statistical analysis

Data are reported as the means ± SD. *P* values ≤ 0.05 were considered statistically significant. One-way analysis of variance (ANOVA) was used to evaluate the effect of the treatments on oxylipins production. When differences were observed, Dunnet's and Bonferroni's multiple comparison tests were used. Statistical analysis was performed using Graph Pad Prism® version 6.00 for Windows (GraphPad Software, Inc., San Diego, CA). The principal component analysis (PCA) projection was performed using the R software package *muma* (Metabolics Univariate and Multivariate analysis), R-statistical open source software (R Core Team (2014). R refers to a language and environment for statistical computing (R Foundation for Statistical Computing, Vienna, Austria. URL http://www.R-project.org/).

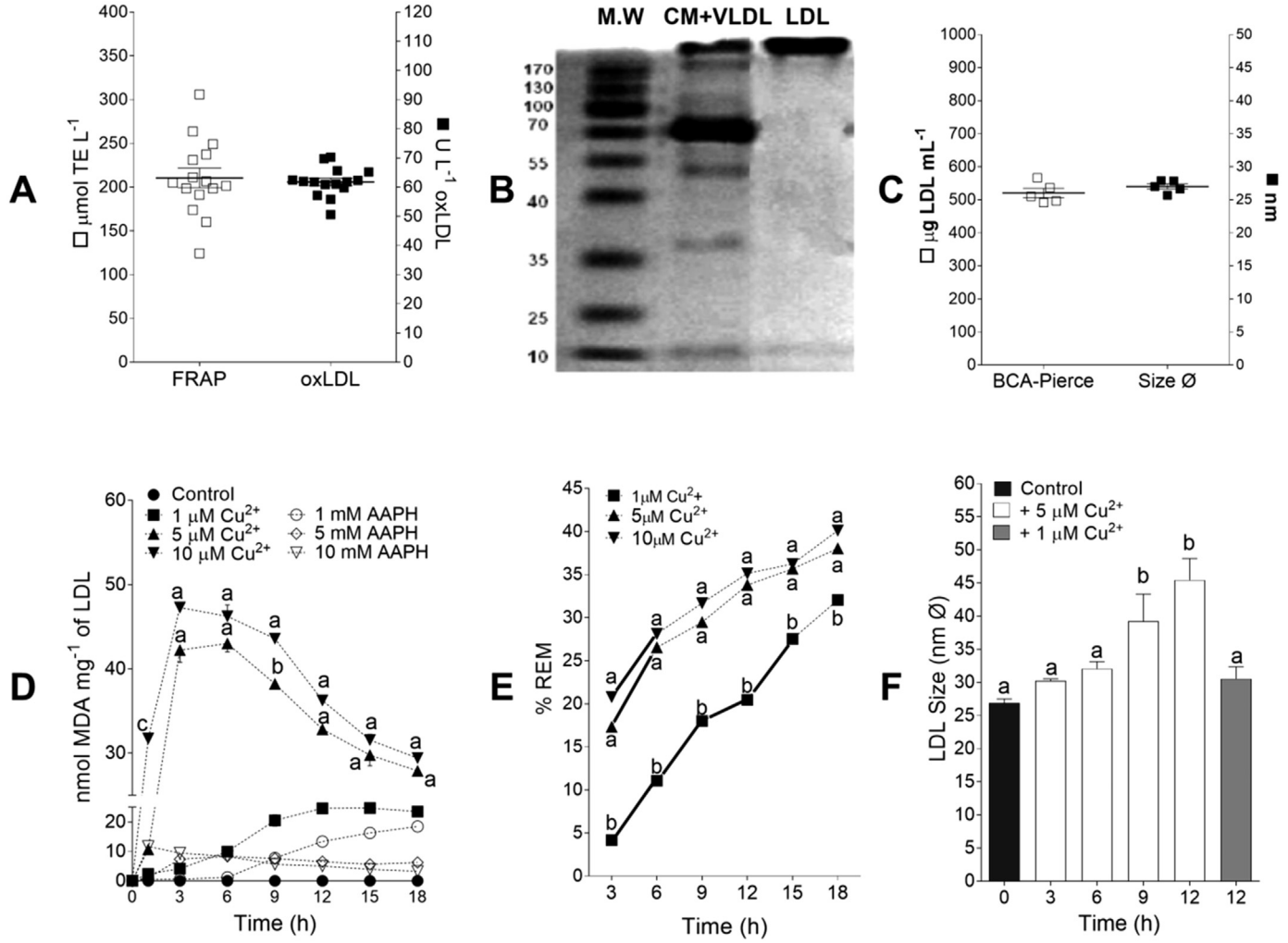

Fig. 1. Physicochemical characterization of oxLDL. A) OxLDL levels are in units per liter (U L^{-1}), and antioxidant capacity is in µmol Trolox equivalents per liter of plasma (µmol TE L^{-1}); n = 15 plasma samples. B) SDS-PAGE of chylomicrons + VLDL (CM + VLDL) and LDL fractions isolated from the plasma pool. C) LDL concentrations in µg mL^{-1} as evaluated by the bicinconinic acid (BCA) method, and LDL size evaluated by dynamic light scattering (DLS). D) nmol MDA mg^{-1} of LDL under copper and AAPH-induced oxidation evaluated by TBARS method[1]. E) Relative electrophoretic mobility (REM) analysis of copper-induced oxLDL expressed as the percentage of electromobility[1]. F) Diameter in nm of oxLDL produced with copper by DLS measurements[2]. Error bars represent the SD. [1] One-way ANOVA; Different letters indicate significant differences in the change values between treatments at the same timepoint (Bonferroni's multiple comparison test, $P < 0.001$). [2] One-way ANOVA; Bars labeled without a common letter differ significantly compared with the control (black bar) (Dunnet's multiple comparison test, $P < 0.001$).

3. Results and discussion

3.1. LDL oxidation and physicochemical characterization

The average plasma antioxidant capacity of 15 subjects according to the FRAP method was 210.55 ± 43.59 µmol TE L^{-1}, and the average oxLDL concentration was 61.76 ± 4.99 U L^{-1} (Fig. 1**A**). According to a previous study, oxLDL concentrations between 51.5 and 76.5 U L^{-1} represent a risk factor for cardiovascular disease (CVD) [36,37]. Currently, there are not clinical reference values for oxLDL in healthy populations; furthermore, the values in the literature differ among the studies [36–38]. The isolated LDL fraction (Fig. 1**B**) was compared with the chylomicrons + VLDL fraction, demonstrating its purity by the presence of a unique apolipoprotein constitutive to LDL, ApoB-100 [39]. Additionally, the concentration of protein evaluated by the BCA method was ~ 500 mg mL^{-1}, and the particle size by DLS was ~ 26 nm (Fig. 1**C**), indicating LDL stability and integrity [40,41].

OxLDL was generated with $CuSO_4$ and AAPH, the most common oxidants used *in vitro* [14,42]. The final selected conditions were 5 µM $CuSO_4$ for 6 h. Although at 10 µM $CuSO_4$ for 3 h, TBARS values were higher (47 nmol MDA mg^{-1} of LDL) and no significant differences were observed with 5 µM $CuSO_4$ at 3 or 6 h ($p > 0.001$) (Fig. 1**D**). Furthermore, reactions longer than 6 h at both concentrations of $CuSO_4$ showed a decrease in TBARS values. By contrast, oxLDL with 1 µM $CuSO_4$ or AAPH (1, 5 and 10 mM) incubated between 0 and 18 h showed only a slight increase in TBARS value, which may correspond to a minimally modified LDL (mmLDL), which is undesirable [43].

Regarding the size, there were no differences in LDL samples treated with 5 µM or 10 µM $CuSO_4$ at all of the time points evaluated ($P > 0.001$) (Fig. 1**E**). However, more than 6 h of incubation endangered the structural integrity of both the lipids and apoB100 in LDL, as confirmed by staining with Sudan black (lipids) and Coomassie blue dyes (proteins) (Fig. 1**S**). From the results mentioned above, we highlight the importance of having a complete oxidation of LDL, as well as guaranteeing the integrity of the particles, to replicate the *in vivo* physiological conditions; an extensive oxidation could produce degradations that make oxLDL not comparable with its *in vivo* analogues. As expected, LDL treated with 1 µM $CuSO_4$ had significantly less relative electrophoretic mobility than LDL treated with 5 µM $CuSO_4$ ($P < 0.001$) without compromising the integrity of LDL, at least over 15 h. In terms of particle size, we observed that oxLDL obtained over 9 h was significantly larger than native LDL and LDL oxidized for 3 and

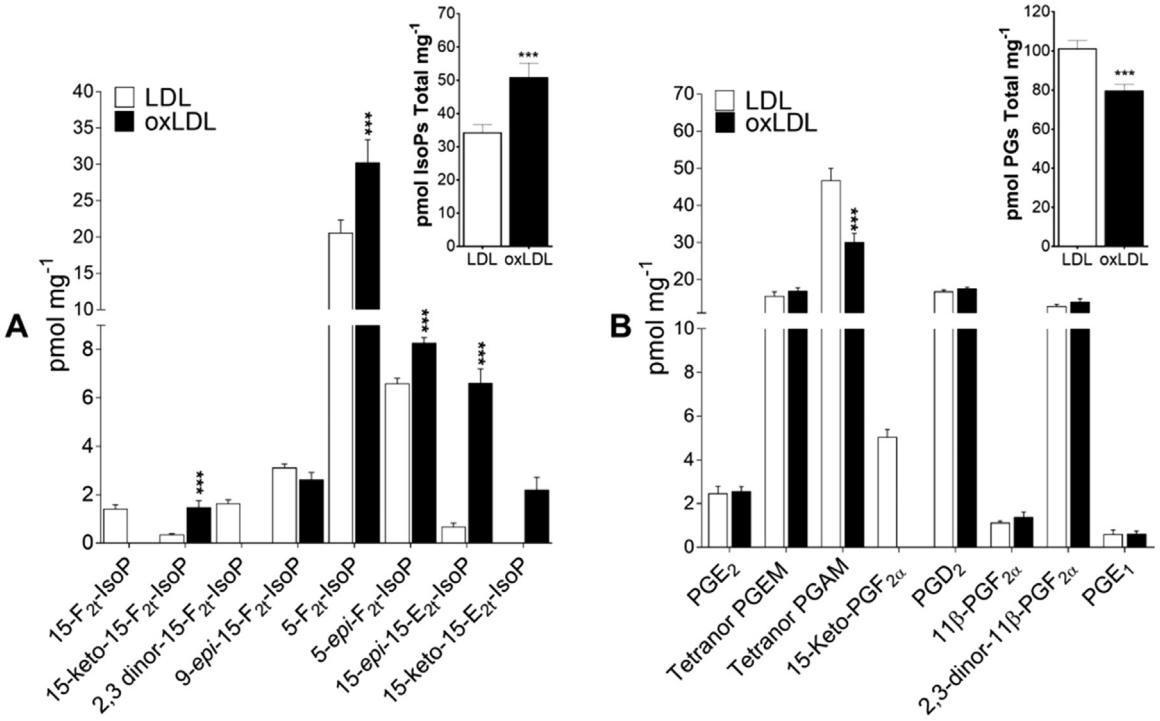

Fig. 2. Oxylipins within LDL and oxLDL expressed as pmol mg^{-1} of protein; A) isoprostanes (IsoPs) and B) prostaglandins (PGs). Bars labeled with * differ significantly (Mann Whitney test, ***$P < 0.0001$). Error bars represent the SD.

6 h ($P < 0.001$) under the optimal conditions. By contrast, oxLDL generated at 12 h with 1 μM $CuSO_4$ did not show structural changes compared to native LDL (Fig. 1**F**). Our results are consistent with those of Oliveira et al., who found that LDL oxidized over 6 h with 10 μM $CuSO_4$ did not show any changes in the dispersity of oxLDL compared with native LDL. Nevertheless, oxLDL obtained by this group at 18 h demonstrated an increase in the size polydispersity of particles [16]. We found polydispersity at 9 and 12 h of oxidation with 5 μM $CuSO_4$, indicating that oxLDL could have formed aggregates, which are artifacts that do not represent real conditions.

3.2. Oxylipin profiles in LDL vs. oxLDL

Of the 14 IsoPs evaluated in native LDL, six F_2-IsoPs and one E_2-IsoP derived from AA were quantified (Fig. 2**A**). We found that 5-F_{2t}-IsoPs (5-F_{2t}-IsoP and 5-*epi*-5-F_{2t}-IsoP) were the most abundant IsoPs, while 15-*epi*-15-E_{2t}-IsoP was the only E_2-IsoP detected. Previous studies have shown that LDL constitutively includes 15-F_{2t}-IsoP (8-*iso* $PGF_{2\alpha}$) in response to normal physiological exposure to oxidative degradation of PUFAs by free radicals in circulation [44,45]. As expected, as a result of oxidation, oxLDL had increased levels of F_{2t}-IsoPs (15-keto-15-F_{2t}-IsoP, 5-F_{2t}-IsoP and 5-*epi*-5-F_{2t}-IsoP) and E_2-IsoPs (15-*epi*-15-E_{2t}-IsoP and 15-keto-15-E_{2t}-IsoP) compared to native LDL ($P < 0.0001$). Despite the marked increase in IsoPs levels in oxLDL due to oxidation, we observed that levels of 15-F_{2t}-IsoP (8-*iso* $PGF_{2\alpha}$) and 2,3-dinor-15-F_{2t}-IsoP were not detected in oxLDL, apparently due to the strong copper-based oxidation, which triggered the formation of new metabolites. Once 15-F_{2t}-IsoP is β-oxidized, it forms an intermediate compound, 2,3-dinor-15-F_{2t}-IsoP that can further undergo reduction to 2,3-dinor-5,6-dihydro-15-F_{2t}-IsoP [46], this compound was not analyzed in our work. However, copper oxidation could lead the formation of 15-keto-15-E_{2t}-IsoP (Scheme 1) which was detected and quantified in oxLDL. Recently, Van'T Erve et al. quantified the formation of 8-iso-$PGF_{2\alpha}$ by enzymatic lipid peroxidation; the *in vitro* experiments were performed with purified prostaglandin-endoperoxide synthases (PGHS) and AA. In the incubations of purified PGHS-1 or −2, no detectable levels of 8-iso-$PGF_{2\alpha}$ were observed. The authors suggest that the undetectable levels of 8-iso-$PGF_{2\alpha}$ were due to a nearly exclusive generation of PGE_2 and other ketone products by spontaneous rearrangement of the endoperoxide intermediates. This does not reflect the *in vivo* conditions, where a reducing environment and enzymes increase the levels of F_2-prostaglandins and F_2-isoprostanes [47]. Therefore, the analysis of 8-iso-$PGF_{2\alpha}$/$PGF_{2\alpha}$ ratio would be suitable for further studies. Several studies have previously reported the presence of F_2- and E_2-IsoPs in plasma [48,49], but data for LDL and oxLDL are limited. To date, previous studies have reported only one epoxyisoprostane (1-palmitoyl-2-(5, 6-epoxyisoprostane E(2))-*sn*-glycero-3-phosphocholine) associated with phospholipids in mmLDL [50], as well as 8-iso-$PGF_{2\alpha}$ in both oxLDL and LDL [44,45,51].

The IsoPs assessed could have vascular properties related to the pro-atherogenic effects of oxLDL. Indeed, Scholz et al. observed that 8-iso-$PGF_{2\alpha}$ augmented oxLDL-induced lipid accumulation of THP-1 macrophages, inducing expression of SRA-1 (at both the mRNA and protein level). Moreover, they also showed that 8-iso-$PGF_{2\alpha}$ counteracted oxLDL-induced apoptosis of macrophages and increased oxLDL-induced gene expression of MMP-9 [52]. These findings further support a role for 8-iso-$PGF_{2\alpha}$ not only as a marker of oxidative stress in patients with atherosclerotic disorders but also as a mediator in atherogenesis and plaque destabilization. Our results provide further evidence supporting the generation of IsoPs in macrophages after OS injury caused by oxLDL.

By contrast, of the 20 PGs evaluated in LDL, four PGE and three PGD metabolites from enzymatic oxidation of AA were quantified (Fig. 2**B**). Among the PGD metabolites, only PGD_2 and those formed by PGF synthesis (PGFS) pathway (the 11β-$PGF_{2\alpha}$ and 2,3-dinor-11β-$PGF_{2\alpha}$ [53]) were detected. In the same way, PGE_2 and its metabolites, such as tetranor-PGEM and tetranor-PGAM [33], as well as 15-keto-$PGF_{2\alpha}$ were detected (the latter was produced from PGE_2 and $PGF_{2\alpha}$ through the hydroxyprostaglandin dehydrogenase (HPGD) pathway [54]). Additionally, among the PGs related to DGLA and EPA enzymatic oxidation, only PGE_1, a well-known anti-inflammatory PG derived from DGLA, was detected [55]. The concentration of the majority of the PGE

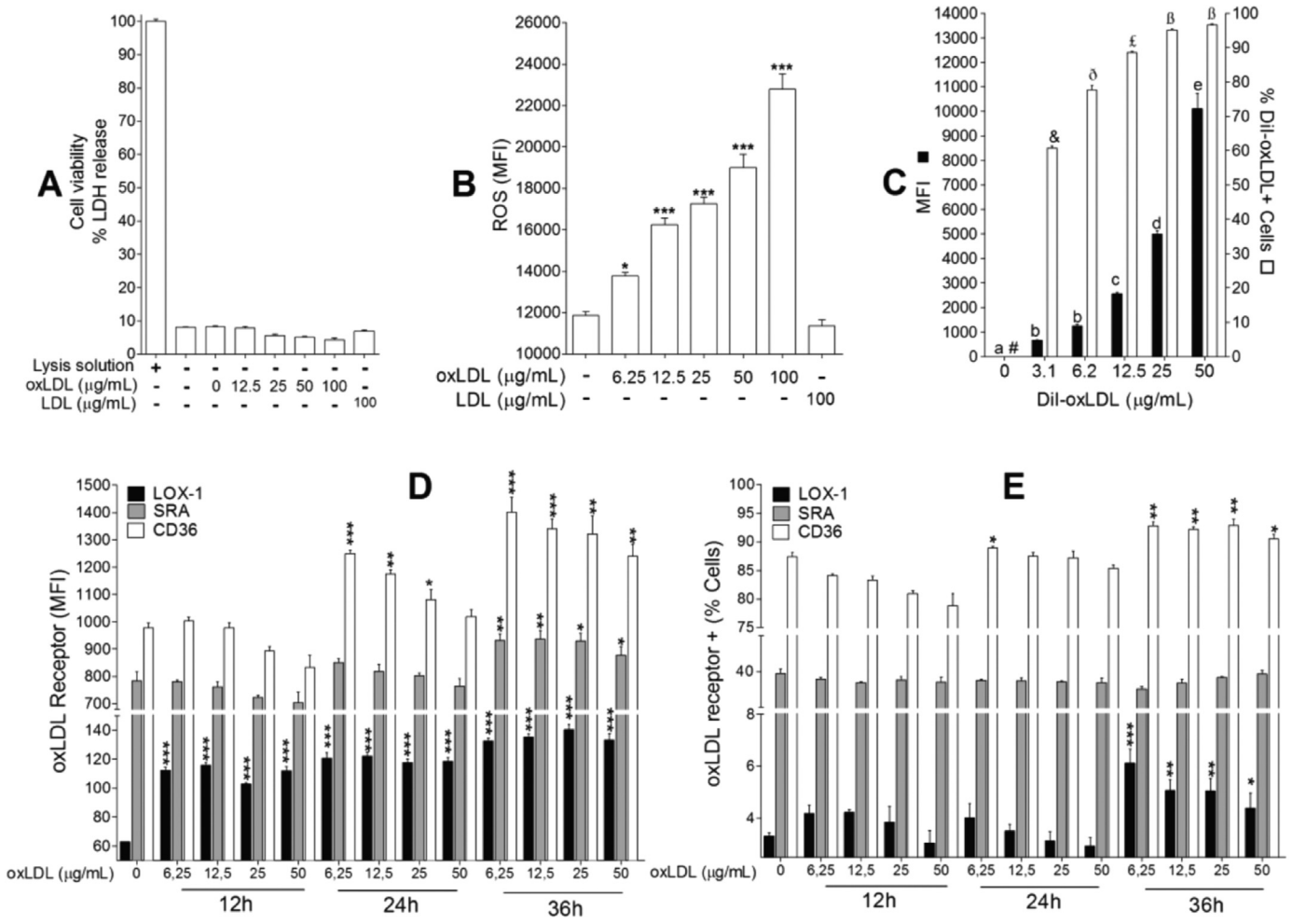

Fig. 3. Cell viability, ROS production, and DiI-oxLDL uptake and expression of proatherogenic receptors on THP-1 macrophages. A) Cell viability. LDH in the media was measured and expressed as a percentage of cell viability. B) Intracellular production of ROS was monitored with a ROS-sensitive fluorescent dye and expressed as MFI[1]. C) DiI-oxLDL uptake by flow cytometry; DiI-oxLDL is reported as the percentage of DiI-oxLDL+ cells and MFI[2]. D and E) Flow cytometry analysis of the oxLDL receptor expression levels in macrophages treated with oxLDL. The levels of receptors are expressed as: D) MFI and E) percentage of CD36+, SR-A+ and LOX-1+ cells[1]. Treatments without oxLDL or DiI-oxLDL are the negative controls. Error bars represent the SD. [1] One-way ANOVA; bars labeled with * differ significantly compared with the negative control (Dunnet's multiple comparison test, *P < 0.05, **P < 0.001 and ***P < 0.001). [2] One-way ANOVA; Different letters or symbols indicate significant differences in the change values (Bonferroni's multiple comparison test, $P < 0.001$).

and PGD metabolites did not change significantly when comparing LDL with oxLDL ($P > 0.05$). The total PGs levels in oxLDL were lower than in LDL (20% and 100% less for tetranor-PGAM and 15-keto-$PGF_{2\alpha}$, respectively; $P < 0.0001$), most likely due to the oxidation mediated by copper. Additionally, PGE_1 did not show differences between both particles, indicating that the original composition of this anti-inflammatory prostaglandin was not altered regardless of the oxidation status of LDL.

3.3. OxLDL induces ROS production and increases expression of oxLDL receptors in THP-1 macrophages

THP-1 macrophages treated with oxLDL for 1 h, at concentrations that did not alter cell viability (6.25–100 μg mL^{-1}) (Fig. 3**A**), increased ROS production by approximately 16% and 92% compared with their basal state in a concentration-dependent fashion ($P < 0.05$). By contrast, LDL treatment did not increase ROS generation in these macrophages (Fig. 3**B**). Previous studies have confirmed this behavior in murine macrophages [32,56,57], showing that ROS production increased over a period of 1–4 h, reaching a plateau at 8 h of oxLDL exposure [56].

The results related to oxLDL uptake by THP-1 macrophages are shown in Fig. 3**C**. DiI-oxLDL is incorporated by THP-1 macrophages in a concentration-dependent fashion. After incubation with 3.125, 6.25, 12.5, 25 and 50 μg mL^{-1}, oxLDL uptake by macrophages significantly increased (664.3 ± 23.86, 1260.80 ± 100.60, 2566.00 ± 80.13, 4993.00 ± 247.00, 10,111.00 ± 1083.13 MFI) compared to the control group (or autofluorescence; 4.0 ± 1.1 ($P < 0.001$)). However, when only cells positive for DiI-oxLDL uptake were evaluated, we did not observe significant differences between 25 μg mL^{-1} and 50 μg mL^{-1}. Finally, the capacity of DiI-oxLDL uptake by macrophages was verified by a competitive assay with unlabeled oxLDL. Co-treatment with DiI-oxLDL and oxLDL decreased the uptake of DiI-oxLDL, indicating that oxLDL was appropriately labeled (Fig. S2A).

CD36, SR-A and LOX-1 are responsible for approximately 90% of oxLDL uptake by macrophages [3,4]. Compared to the basal state, expression of CD36 significantly increased after 24 h ($P < 0.05$) except at 50 μg mL^{-1} and 36 h ($P < 0.001$) of treatment with oxLDL (Fig. 3**D**). This receptor expression increased in a time-dependent manner but was independent of the oxLDL concentration. Despite the increase in CD36 expression, the percentage of CD36-positive cells only increased significantly after 36 h at low concentrations of oxLDL (Fig. 3**E**; CD36+). In contrast to CD36, compared to the basal state, SR-A expression significantly increased after 36 h of oxLDL treatment ($P < 0.05$) (Fig. 3**D**).

The percentage of SR-A-positive cells remained unaltered with oxLDL treatment ($P > 0.05$) (Fig. 3**E**). On the other hand, induction of LOX-1 expression by oxLDL on THP-1 macrophages was significantly higher compared to the basal state at all timepoints and concentration treatments ($P < 0.001$) (Fig. 3**D and E**). However, the percentage of LOX-1 + macrophages only increased significantly after 36 h of treatment. Similar to CD36 analysis, the LOX-1 levels increased in a time-dependent manner but were independent of the oxLDL concentration. In general, oxLDL strongly induced oxLDL receptors after 36 h, according to both their expression levels and the percentages of cells with these receptors.

Previous studies have also shown the induction effect of oxLDL on CD36, SR-A and LOX-1 in macrophages [58,59]. However, only CD36 and SR-A were induced in murine macrophages (RAW264.7) by using commercial oxLDL for 24 h [58], whereas in human macrophages, oxLDL at 18 h induced both CD36 and LOX-1, with a positive correlation with proinflammatory mediators and negative correlation with SR-A [59]. Our results showed a significant induction of SR-A mediated by oxLDL after 36 h of exposure. Finally, contrary to the induction effect of oxLDL, native LDL significantly attenuated CD36, SR-A and LOX-1 protein expression ($P < 0.001$) (Figs. S2B and S2C). Our results confirm that native LDL is not involved in foam cell formation.

3.4. LDL/oxLDL-macrophage interactions and oxylipin profiles

Incubation of THP-1 macrophages with LDL and oxLDL triggered substantial changes in oxylipin profiles; the overall results after treatment with LDL or oxLDL, both in cells and in culture supernatants, at 1, 6 and 12 h are summarized in Fig. S3. Of the 34 oxylipins evaluated, 20 were detected: ten PGs (PGE_2, tetranor–PGEM, tetranor–PGAM, 15-keto-PGF2α, PGD_2, 11β-$PGF_{2\alpha}$, PGDM, tetranor-PGDM, PGE_1 and 17-*trans*-$PGF_{3\alpha}$), and ten IsoPs (15-F_{2t}-IsoP, 15-keto-15-F_{2t}-IsoP, 2,3-dinor-15-F_{2t}-IsoP, 9-*epi*-15-F_{2t}-IsoP, $PGF_{2\alpha}$, 5-F_{2t}-IsoPs, 5-*epi*-5-F_{2t}-IsoP, 15-*epi*-15-E_{2t}-IsoP, 15-E_{1t}-IsoP and 8-F_{3t}-IsoP).

3.4.1. Oxylipin levels in supernatants

Regarding prostaglandins, PGDM, tetranor-PGDM, 17-*trans*-$PGF_{3\alpha}$ were produced exclusively after macrophages were stimulated with oxLDL and were not detected either in the control (macrophages at basal state with no treatment) or after treatment with LDL. All PGE metabolites released into the medium were strongly increased by oxLDL treatment. The IsoPs not linked to phospholipids produced exclusively from oxLDL treatment were 15-keto-15-F_{2t}-IsoP, 15-E_{1t}-IsoP and 8-F_{3t}-IsoP. Although 15-F_{2t}-IsoP, 5-F_{2t}-IsoP, *epi*-5-F_{2t}-IsoP and 15-*epi*-15-E_{2t}-IsoP were highly produced after oxLDL treatment, they were also generated with LDL stimulation, albeit in lesser amounts (Tables S2 and S3).

3.4.2. Cellular oxylipin levels

Regarding prostaglandins, the levels of PGDM, tetranor-PGDM, 17-*trans*-$PGF_{3\alpha}$ were measured exclusively in macrophages after oxLDL stimulation and were not detected in the controls or after LDL treatment. PGE_2 and PGD_2 were not detected in cells. By contrast, all of the PGE_2 and PGD_2 metabolites were quantified at high concentrations in cells after oxLDL treatment. Regarding IsoPs, 15-*epi*-15-E_{2t}-IsoP, 15-E_{1t}-IsoP, and 8-F_{3t}-IsoP were quantified exclusively after macrophages were stimulated with oxLDL. Although high concentrations of 15-F_{2t}-IsoP, 5-F_{2t}-IsoP and 5-*epi*-5-F_{2t}-IsoP were detected after oxLDL treatments, these were also detected to a lesser extent with LDL stimulation and in the basal state.

3.5. Biomarkers of oxidative stress and inflammation

The oxylipin composition of macrophages treated with LDL and oxLDL were comprehensively examined using PCA (Fig. 4**A**). The Score plot revealed three discrete clusters, which have been circled and labeled as: C1, macrophages treated with LDL at all concentrations and time points; C2, macrophages in the basal state (control) and after exposure to oxLDL at different concentrations but only in experiments at 1 h; and C3, macrophages stimulated with oxLDL at 6 and 12 h (Fig. 4**A**). The three different zones resulted from plotting principal components 1 and 2, which accounted for approximately 56.4% of the total variation. The loading plots of the first principal components show that the oxidative stress marker,5-*epi*-5-F_{2t}-IsoP, 15-E_{1t}-IsoP, 8-F_{3t}-IsoP and 15-keto-15-F_{2t}-IsoP, as well as the inflammatory markers PGDM, 17-*trans*-$PGF_{3\alpha}$, and 11β-$PGF_{2\alpha}$, are the main metabolites responsible for the THP-1-macrophage response to oxLDL exposure (C3) at high concentrations and after 6 and 12 h of treatment ($P < 0.05$) (Fig. 4**B**). Remarkably, 5-*epi*-5-F_{2t}-IsoP was the oxidative stress marker with the highest level of production in macrophages with oxLDL exposure for 6 and 12 h. The concentration of PGDM after stimulation by oxLDL (6 and 12 h) was between 57% and 90% of the total PGs quantified. On the other hand, tetranor-PGAM, tetranor-PGEM and PGE_1 were produced

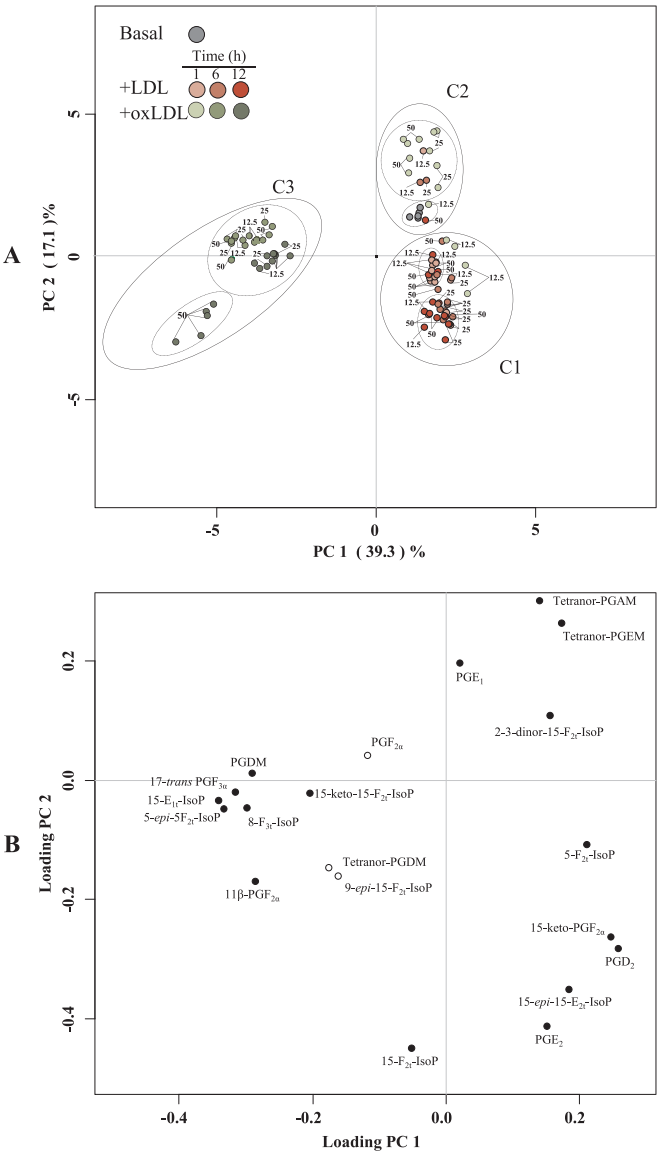

Fig. 4. Oxylipins in culture medium after oxLDL and LDL stimulation of THP-1 macrophages. A) Principal component analysis (PC1 vs. PC2) of the THP-1 macrophage response to oxLDL and LDL treatments (12.5, 25 and 50 μg mL^{-1} for 1, 6 and 12 h), and B) the corresponding loading plot. The combination of PC1-PC2 analysis shows clustering of macrophages related to their ability to produce and excrete oxylipins. Five replicates for each sample were used. Filled black circles indicate P values < 0.05.

mainly with oxLDL treatment for 1 h ($P < 0.05$) (C2), while PGE_2, PGD_2, 15-keto-$PGF_{2\alpha}$ 15-*epi*-15-E_{2t}-IsoP and 5-F_{2t}-IsoP were the main metabolites responsible for the THP-1-macrophage response to LDL exposure ($P < 0.05$) (C1).

Similar to our results, previous studies have reported an induction effect of LDL on PGE_2, PGD_2 and $PGF_{2\alpha}$ [60,61], suggesting a possible contribution to the inflammatory process in the arterial wall related to native LDL. Additionally, PGE_1 and 17-*trans*-$PGF_{3\alpha}$ (a double-bond isomer of $PGF_{3\alpha}$), which are recognized as anti-inflammatory molecules [62,63], were also detected and quantified in supernatants. PGE_1 was not significantly induced by LDL treatment, but was significantly induced by oxLDL (Fig. 4**B**), which suggests an anti-inflammatory response to injury caused by oxLDL after 1 h of exposure. On the other hand, 17-*trans*-$PGF_{3\alpha}$ was only detected when macrophages were exposed to oxLDL. This anti-inflammatory response suggests that the foam cells express salvage pathways to alleviate the cytotoxicity and inflammation generated by cholesterol-loading in macrophages [5,64]. As shown in Fig. 4, the PCA loading plot indicates that 17-*trans*-$PGF_{3\alpha}$ alone is the main prostaglandin with an anti-inflammatory profile responsible for the macrophage response to high concentrations and prolonged exposure to oxLDL (Fig. 4; 6 and 16 h; C3), whereas PGE_1 is closely related to short oxLDL treatment (Fig. 4; 1 h; C2). PGE_1 is a potent vasodilator and inhibitor of platelet aggregation and is recognized as a smooth muscle relaxant [65], whereas the beneficial effects of the 3-series oxylipins have been more gradually clarified. $PGF_{3\alpha}$ has demonstrated anti-inflammatory effect [63,66], and 17-*trans*-$PGF_{3\alpha}$ is an indicator of its production.

The biological effects of IsoPs are still a matter of active research; in general, they are consistently described as pro-inflammatory and vasoconstriction mediators [11] as well as biomarkers of clinical pathologies, including asthma, CVD, risk factors of atherosclerosis, chronic obstructive pulmonary diseases, diabetes, ischemia-reperfusion, rheumatic diseases and aseptic shock [10,11]. Additionally, several may have regulatory effects [67]. To date, our study is the first to analyzing IsoPs individually and that result from oxLDL-mediated OS injury in THP-1 macrophages.

4. Conclusions

In this study, we establish the potent impact of oxLDL on the oxylipin profiles of THP-1 human macrophages, as well as on key relevant events, including oxLDL uptake, oxLDL receptor expression and ROS production. We show that oxLDL specifically induces biomarkers related to oxidation, such as 5-*epi*-5-F_{2t}-IsoP, 15-E_{1t}-IsoP, 8-F_{3t}-IsoP and 15-keto-15-F_{2t}-IsoP, as well as the inflammatory markers PGDM, 17-*trans*-$PGF_{3\alpha}$, 11β-$PGF_{2\alpha}$, all of which are reported for the first time in this *in vitro* model. Additionally, PGE_1 and 17-*trans*-$PGF_{3\alpha}$, two recognized anti-inflammatory molecules, were also detected for the first time in this model. This anti-inflammatory response suggests that foam cells express salvage pathways to alleviate cytotoxicity and inflammation. Finally, this comprehensive characterization of the interaction between oxLDL and macrophages contributes to our understanding of the initial atherogenic events mediated by oxylipins and provides insights into developing new approaches for their potential therapeutic modulation.

Acknowledgements

The authors thank the volunteers who provided the LDL. The authors are grateful for the support of COLCIENCIAS through grant no. 528-2011 for doctoral students, the young researchers and innovators program (617–2013) and to the “Fundación Séneca de la Región de Murcia” Grupo de Excelencia 19900/GERM/15. This work is included in the framework of the collaboration between the Spanish Research Council (CEBAS-CSIC) and CNRS by “Projets Internationaux de Cooperation Scientifique (PICS-2015–261141). They also thank the Ibero-American Programme for Science, Technology and Development (CYTED) – Action 112RT0460 CORNUCOPIA and the project i-link 0846 (i-Link + 2013 CSIC). Finally, KM-D and OJL-G thank to Dr. Juan Escobar for his help with R software.

Conflicts of interest

KM-D and OJL-G are researchers at the Vidarium, Nutrition, Health and Wellness Research Center, Nutresa Business Group. NZ, RA-Q, EO AG-I, SM, CO, TD and J-MG state that they have no conflicts of interest.

Appendix A. Supporting information

Supplementary data associated with this article can be found in the online version at http://dx.doi.org/10.1016/j.redox.2017.11.017.

References

[1] T. Gui, A. Shimokado, Y. Sun, T. Akasaka, Y. Muragaki, Diverse roles of macrophages in atherosclerosis: from inflammatory biology to biomarker discovery, Mediat. Inflamm. 2012 (2012), http://dx.doi.org/10.1155/2012/693083.
[2] D. Steinberg, The LDL modification hypothesis of atherogenesis: an update, J. Lipid Res. 50 (2009) S376–S381, http://dx.doi.org/10.1194/jlr.R800087-JLR200.
[3] V.V. Kunjathoor, M. Febbraio, E.A. Podrez, K.J. Moore, L. Andersson, S. Koehn, J.S. Rhee, R. Silverstein, H.F. Hoff, M.W. Freeman, Scavenger receptors class A-I/II and CD36 are the principal receptors responsible for the uptake of modified low density lipoprotein leading to lipid loading in macrophages, J. Biol. Chem. 277 (2002) 49982–49988, http://dx.doi.org/10.1074/jbc.M209649200.
[4] A. Pirillo, G.D. Norata, A.L. Catapano, LOX-1, OxLDL, and atherosclerosis, Mediat. Inflamm. 2013 (2013) 12, http://dx.doi.org/10.1155/2013/152786.
[5] K.J. Moore, I. Tabas, Macrophages in the pathogenesis of atherosclerosis, Cell 145 (2011) 341–355, http://dx.doi.org/10.1016/j.cell.2011.04.005.
[6] W. Liu, Y. Yin, Z. Zhou, M. He, Y. Dai, OxLDL-induced IL-1beta secretion promoting foam cells formation was mainly via CD36 mediated ROS production leading to NLRP3 inflammasome activation, Inflamm. Res. 63 (2014) 33–43, http://dx.doi.org/10.1007/s00011-013-0667-3.
[7] S. Gleim, J. Stitham, W.H. Tang, K.A. Martin, J. Hwa, An eicosanoid-centric view of atherothrombotic risk factors, Cell. Mol. Life Sci. 69 (2012) 3361–3380, http://dx.doi.org/10.1007/s00018-012-0982-9.
[8] L.J. Roberts II, J.D. Morrow, Products of the isoprostane pathway: unique bioactive compounds and markers of lipid peroxidation, Cell. Mol. Life Sci. 59 (2002), http://dx.doi.org/10.1007/s00018-002-8469-8.
[9] C. Vigor, J. Bertrand-Michel, E. Pinot, C. Oger, J. Vercauteren, P. Le Faouder, J.-M. Galano, J.C.-Y. Lee, T. Durand, Non-enzymatic lipid oxidation products in biological systems: assessment of the metabolites from polyunsaturated fatty acids, J. Chromatogr. B 964 (2014) 65–78, http://dx.doi.org/10.1016/j.jchromb.2014.04.042.
[10] S. Basu, Bioactive eicosanoids: role of prostaglandin F2α and F2-isoprostanes in inflammation and oxidative stress related pathology, Mol. Cells 30 (2010) 383–391, http://dx.doi.org/10.1007/s10059-010-0157-1.
[11] G.L. Milne, H. Yin, K.D. Hardy, S.S. Davies, L.J. Roberts, Isoprostane generation and function, Chem. Rev. 111 (2011) 5973–5996, http://dx.doi.org/10.1021/cr200160h.
[12] S. Medina, R. Domínguez-Perles, J.I. Gil, F. Ferreres, A. Gil-Izquierdo, Metabolomics and the diagnosis of human diseases – a guide to the markers and pathophysiological pathways affected, Curr. Med. Chem. 21 (2014), http://dx.doi.org/10.2174/092986732066131119124056.
[13] V. Capra, M. Bäck, S.S. Barbieri, M. Camera, E. Tremoli, G.E. Rovati, Eicosanoids and their drugs in cardiovascular diseases: focus on atherosclerosis and stroke, Med. Res. Rev. 33 (2013) 364–438, http://dx.doi.org/10.1002/med.21251.
[14] I. Levitan, S. Volkov, P.V. Subbaiah, Oxidized LDL: diversity, patterns of recognition, and pathophysiology, Antioxid. Redox Signal. 13 (2010) 39–75, http://dx.doi.org/10.1089/ars.2009.2733.
[15] K. Öörni, M.O. Pentikäinen, A. Annila, P.T. Kovanen, Oxidation of low density lipoprotein particles decreases their ability to bind to human aortic proteoglycans. Dependence on oxidative modification of the lysine residues, J. Biol. Chem. 272 (1997) 21303–21311, http://dx.doi.org/10.1074/jbc.272.34.21303.
[16] C.L.P. Oliveira, P.R. Santos, A.M. Monteiro, A.M. Figueiredo Neto, Effect of oxidation on the structure of human low- and high-density lipoproteins, Biophys. J. 106 (2014) 2595–2605, http://dx.doi.org/10.1016/j.bpj.2014.04.049.
[17] A. Kontush, M.J. Chapman, Lipidomics as a tool for the study of lipoprotein metabolism, Curr. Atheroscler. Rep. 12 (2010) 194–201, http://dx.doi.org/10.1007/s11883-010-0100-0.
[18] C. Mesaros, S.H. Lee, I.A. Blair, Targeted quantitative analysis of eicosanoid lipids in biological samples using liquid chromatography-tandem mass spectrometry, J. Chromatogr. B. Anal. Technol. Biomed. Life Sci. 877 (2009) 2736–2745, http://dx.doi.org/10.1016/j.jchromb.2009.03.011.
[19] P.C. Norris, E.A. Dennis, A lipidomic perspective on inflammatory macrophage eicosanoid signaling, Adv. Biol. Regul. 54 (2014) 99–110, http://dx.doi.org/10.1016/j.jbior.2013.09.009.

[20] N.J. Spann, C.K. Glass, Sterols and oxysterols in immune cell function, Nat. Immunol. 14 (2013), http://dx.doi.org/10.1038/ni.2681.

[21] K. Ekroos, M. Jänis, K. Tarasov, R. Hurme, R. Laaksonen, Lipidomics: a tool for studies of atherosclerosis, Curr. Atheroscler. Rep. 12 (2010) 273–281, http://dx.doi.org/10.1007/s11883-010-0110-y.

[22] S. Medina, R. Domínguez-Perles, J.I. Gil, F. Ferreres, C. García-Viguera, J.M. Martínez-Sanz, A. Gil-Izquierdo, A ultra-pressure liquid chromatography/triple quadrupole tandem mass spectrometry method for the analysis of 13 eicosanoids in human urine and quantitative 24h values in healthy volunteers in a controlled constant diet, Rapid Commun. Mass Spectrom. 26 (2012) 1249–1257, http://dx.doi.org/10.1002/rcm.6224.

[23] T. Durand, J.L. Cracowski, A. Guy, J.C. Rossi, Syntheses and preliminary pharmacological evaluation of the two epimers of the 5-F2t-isoprostane, Bioorg. Med Chem. Lett. 11 (2001) 2495–2498 (doi:S0960-894X)(01)(00473-5)(pii).

[24] T. Durand, A. Guy, O. Henry, J.-P. Vidal, J.-C. Rossi, C. Rivalta, A. Valagussa, C. Chiabrando, Total syntheses of four metabolites of 15-F2t-isoprostane, Eur. J. Org. Chem. 2001 (2001) 809–819, http://dx.doi.org/10.1002/1099-0690(200102)2001:4<809::aid-ejoc809>3.0.co;2-6.

[25] C. Oger, Y. Brinkmann, S. Bouazzaoui, T. Durand, J.M. Galano, Stereocontrolled access to isoprostanes via a bicyclo[3.3.0]octene framework, Org. Lett. 10 (2008) 5087–5090, http://dx.doi.org/10.1021/ol802104z (doi).

[26] Y. Brinkmann, C. Oger, A. Guy, T. Durand, J.-M. Galano, Total synthesis of 15-D2t- and 15-epi-15-E2t-isoprostanes, J. Org. Chem. 75 (2010) 2411–2414, http://dx.doi.org/10.1021/jo1000274.

[27] A. Guy, C. Oger, J. Heppekausen, C. Signorini, C. De Felice, A. Furstner, T. Durand, J.M. Galano, Oxygenated metabolites of n-3 polyunsaturated fatty acids as potential oxidative stress biomarkers: total synthesis of 8-F3t-IsoP, 10-F4t-NeuroP and [D4] − 10-F4t-NeuroP, Chem. (Easton). 20 (2014) 6374–6380, http://dx.doi.org/10.1002/chem.201400380 (doi).

[28] G.M. Agudelo-Ochoa, I.C. Pulgarín-Zapata, C.M. Velásquez-Rodriguez, M. Duque-Ramírez, M. Naranjo-Cano, M.M. Quintero-Ortiz, O.J. Lara-Guzmán, K. Muñoz-Durango, Coffee consumption increases the antioxidant capacity of plasma and has no effect on the lipid profile or vascular function in healthy adults in a randomized controlled trial, J. Nutr. 146 (2016) 524–531, http://dx.doi.org/10.3945/jn.115.224774.

[29] O.J. Lara-Guzmán, R. Álvarez-Quintero, E. Osorio, M. Naranjo-Cano, K. Muñoz-Durango, GC/MS method to quantify bioavailable phenolic compounds and antioxidant capacity determination of plasma after acute coffee consumption in human volunteers, Food Res. Int. (2016), http://dx.doi.org/10.1016/j.foodres.2016.07.020.

[30] N. Jiménez, L. Carrillo-Hormaza, A. Pujol, F. Álzate, E. Osorio, O. Lara-Guzman, Antioxidant capacity and phenolic content of commonly used anti-inflammatory medicinal plants in Colombia, Ind. Crops Prod. 70 (2015) 272–279, http://dx.doi.org/10.1016/j.indcrop.2015.03.050.

[31] O.V. Vieira, J.A.N. Laranjinha, V.M.C. Madeira, L.M. Almeida, Rapid isolation of low density lipoproteins in a concentrated fraction free from water-soluble plasma antioxidants, J. Lipid Res. 37 (1996) 2715–2721 〈http://www.scopus.com/inward/record.url?eid=2-s2.0-0030481795&partnerID=40&md5=0851f42092d87248b6fef79590b57115〉.

[32] O.J. Lara-Guzman, J.H. Tabares-Guevara, Y.M. Leon-Varela, R.M. Álvarez, M. Roldan, J.A. Sierra, J.A. Londoño-Londõno, J.R. Ramirez-Pineda, Proatherogenic macrophage activities are targeted by the flavonoid quercetin, J. Pharmacol. Exp. Ther. 343 (2012), http://dx.doi.org/10.1124/jpet.112.196147.

[33] E. Moita, A. Gil-Izquierdo, C. Sousa, F. Ferreres, L.R. Silva, P. Valentão, R. Domínguez-Perles, N. Baenas, P.B. Andrade, Integrated analysis of COX-2 and iNOS derived inflammatory mediators in LPS-Stimulated RAW macrophages pre-exposed to Echium plantagineum L. Bee Pollen Extract, PLoS One 8 (2013), http://dx.doi.org/10.1371/journal.pone.0059131.

[34] S. Medina, R. Domínguez-Perles, R. Cejuela-Anta, D. Villaño, J.M. Martínez-Sanz, P. Gil, C. García-Viguera, F. Ferreres, J.I. Gil, A. Gil-Izquierdo, Assessment of oxidative stress markers and prostaglandins after chronic training of triathletes, Prostaglandins Other Lipid Mediat. (2012), http://dx.doi.org/10.1016/j.prostaglandins.2012.07.002.

[35] A. Kuksis, W. Pruzanski, Hydrolysis of phosphatidylcholine-isoprostanes (PtdCho-IP) by peripheral human group IIA, V and X secretory phospholipases A2 (sPLA2), Lipids 52 (2017) 477–488, http://dx.doi.org/10.1007/s11745-017-4264-z.

[36] L.E. Ramos-Arellano, J.F. Muñoz-Valle, U. De la Cruz-Mosso, A.B. Salgado-Bernabé, N. Castro-Alarcón, I. Parra-Rojas, Circulating CD36 and oxLDL levels are associated with cardiovascular risk factors in young subjects, BMC Cardiovasc. Disord. 14 (2014), http://dx.doi.org/10.1186/1471-2261-14-54.

[37] T. Wu, W.C. Willett, N. Rifai, I. Shai, J.E. Manson, E.B. Rimm, Is plasma oxidized low-density lipoprotein, measured with the widely used antibody 4E6, an independent predictor of coronary heart disease Among U.S. Men and Women? J. Am. Coll. Cardiol. 48 (2006) 973–979, http://dx.doi.org/10.1016/j.jacc.2006.03.057.

[38] J.Y. Kim, J.Y. Park, H.J. Kang, O.Y. Kim, J.H. Lee, Beneficial effects of Korean red ginseng on lymphocyte DNA damage, antioxidant enzyme activity, and LDL oxidation in healthy participants: a randomized, double-blind, placebo-controlled trial, Nutr. J. 11 (2012) 47, http://dx.doi.org/10.1186/1475-2891-11-47.

[39] H.N. Ginsberg, Lipoprotein physiology, Endocrinol. Metab. Clin. North Am. 27 (1998) 503–519, http://dx.doi.org/10.1016/s0889-8529(05)70023-2.

[40] C.L.P. Oliveira, P.R. Santos, A.M. Monteiro, A.M. Figueiredo Neto, Effect of oxidation on the structure of human low- and high-density lipoproteins, Biophys. J. 106 (2014) 2595–2605, http://dx.doi.org/10.1016/j.bpj.2014.04.049.

[41] S. Trirongjitmoah, T. Sakurai, K. Iinaga, H. Chiba, K. Shimizu, Fraction estimation of small, dense LDL using autocorrelation function of dynamic light scattering, Opt. Express 18 (2010) 6315–6326, http://dx.doi.org/10.1364/oe.18.006315.

[42] H. Yoshida, R. Kisugi, Mechanisms of LDL oxidation, Clin. Chim. Acta 411 (2010) 1875–1882, http://dx.doi.org/10.1016/j.cca.2010.08.038.

[43] H. Itabe, M. Mori, Y. Fujimoto, Y. Higashi, T. Takano, Minimally modified LDL is an oxidized LDL enriched with oxidized phosphatidylcholines, J. Biochem. 134 (2003) 459–465, http://dx.doi.org/10.1093/jb/mvg164.

[44] S.M. Lynch, J.D. Morrow, L.J. Roberts 2nd, B. Frei, Formation of non-cyclooxygenase-derived prostanoids (F2-isoprostanes) in plasma and low density lipoprotein exposed to oxidative stress in vitro, J. Clin. Invest. 93 (1994) 998–1004, http://dx.doi.org/10.1172/JCI117107.

[45] N.K. Gopaul, J. Nourooz-Zadeh, A.I. Mallet, E.E. Anggard, Formation of F2-isoprostanes during aortic endothelial cell-mediated oxidation of low density lipoprotein, FEBS Lett. 348 (1994) 297–300.

[46] J.-M. Galano, Y.Y. Lee, C. Oger, C. Vigor, J. Vercauteren, T. Durand, M. Giera, J.C.-Y. Lee, , Isoprostanes, neuroprostanes and phytoprostanes: an overview of 25years of research in chemistry and biology, Prog. Lipid Res. 68 (2017) 83–108, http://dx.doi.org/10.1016/j.plipres.2017.09.004.

[47] T.J. Van'T Erve, F.B. Lih, M.B. Kadiiska, L.J. Deterding, T.E. Eling, R.P. Mason, Reinterpreting the best biomarker of oxidative stress: the 8-iso-PGF2α/PGF2α ratio distinguishes chemical from enzymatic lipid peroxidation, Free Radic. Biol. Med. (2015), http://dx.doi.org/10.1016/j.freeradbiomed.2015.03.004.

[48] H.C. Yen, T.W. Chen, T.C. Yang, H.J. Wei, J.C. Hsu, C.L. Lin, Levels of F2-isoprostanes, F4-neuroprostanes, and total nitrate/nitrite in plasma and cerebrospinal fluid of patients with traumatic brain injury, Free Radic. Res. 49 (2015) 1419–1430, http://dx.doi.org/10.3109/10715762.2015.1080363.

[49] J.D. Morrow, T.A. Minton, C.R. Mukundan, M.D. Campbell, W.E. Zackert, V.C. Daniel, K.F. Badr, I.A. Blair, L.J. Roberts 2nd, Free radical-induced generation of isoprostanes in vivo. Evidence for the formation of D-ring and E-ring isoprostanes, J. Biol. Chem. 269 (1994) 4317–4326.

[50] A.D. Watson, G. Subbanagounder, D.S. Welsbie, K.F. Faull, M. Navab, M.E. Jung, A.M. Fogelman, J.A. Berlinert, Structural identification of a novel pro-inflammatory epoxyisoprostane phospholipid in mildly oxidized low density lipoprotein, J. Biol. Chem. 274 (1999) 24787–24798, http://dx.doi.org/10.1074/jbc.274.35.24787.

[51] K.P. Moore, V. Darley-Usmar, J. Morrow, L.J. Roberts 2nd, Formation of F2-isoprostanes during oxidation of human low-density lipoprotein and plasma by peroxynitrite, Circ. Res. 77 (1995) 335–341.

[52] H. Scholz, P. Aukrust, J.K. Damas, S. Tonstad, E.L. Sagen, S.O. Kolset, C. Hall, A. Yndestad, B. Halvorsen, 8-isoprostane increases scavenger receptor A and matrix metalloproteinase activity in THP-1 macrophages, resulting in long-lived foam cells, Eur. J. Clin. Invest. 34 (2004) 451–458, http://dx.doi.org/10.1111/j.1365-2362.2004.01376.x.

[53] B.L. Dozier, K. Watanabe, D.M. Duffy, Two pathways for prostaglandin F2α (PGF2α) synthesis by the primate periovulatory follicle, Reproduction 136 (2008) 53–63, http://dx.doi.org/10.1530/rep-07-0514.

[54] D. Lu, C. Han, T. Wu, 15-hydroxyprostaglandin dehydrogenase-derived 15-Keto-prostaglandin E(2) inhibits cholangiocarcinoma cell growth through interaction with peroxisome proliferator-activated receptor-γ, SMAD2/3, and TAP63 proteins, J. Biol. Chem. 288 (2013) 19484–19502, http://dx.doi.org/10.1074/jbc.M113.453886.

[55] A. Ahluwalia, M. Perretti, Anti-inflammatory effect of prostanoids in mouse and rat skin: evidence for a role of EP3-receptors, J. Pharmacol. Exp. Ther. 268 (1994) 1526–1531 〈http://jpet.aspetjournals.org/content/268/3/1526.abstract〉.

[56] S.J. Lee, C.H.T. Quach, K.H. Jung, J.Y. Paik, J.H. Lee, J.W. Park, K.H. Lee, Oxidized low-density lipoprotein stimulates macrophage 18F-FDG uptake via hypoxia-inducible factor-1α activation through Nox2-dependent reactive oxygen species generation, J. Nucl. Med. 55 (2014) 1699–1705, http://dx.doi.org/10.2967/jnumed.114.139428.

[57] J.H. Tabares-Guevara, O.J. Lara-Guzmán, J.A. Londoño-Londoño, J.A. Sierra, Y.M. León-Varela, R.M. álvarez-Quintero, E.J. Osorio, J.R. Ramirez-Pineda, Natural biflavonoids modulate macrophage-oxidized LDL interaction in vitro and promote atheroprotection in vivo, Front. Immunol. 8 (2017), http://dx.doi.org/10.3389/fimmu.2017.00923.

[58] M. Crucet, S.J.A. Wüst, P. Spielmann, T.F. Lüscher, R.H. Wenger, C.M. Matter, Hypoxia enhances lipid uptake in macrophages: role of the scavenger receptors Lox1, SRA, and CD36, Atherosclerosis 229 (2013) 110–117, http://dx.doi.org/10.1016/j.atherosclerosis.2013.04.034.

[59] P. Martín-Fuentes, F. Civeira, D. Recalde, A.L. García-Otín, E. Jarauta, I. Marzo, A. Cenarro, Individual variation of scavenger receptor expression in human macrophages with oxidized low-density lipoprotein is associated with a differential inflammatory response, J. Immunol. 179 (2007) 3242–3248, http://dx.doi.org/10.4049/jimmunol.179.5.3242.

[60] D. Jambou, N. Dejour, P. Bayer, J.-C. Poirée, A. Frédenrich, M. Issa-Sayegh, M. Adjovi-Desouza, P. Lapalus, M. Harter, Effect of human native low-density and high-density lipoproteins on prostaglandin production by mouse macrophage cell line P388D1: possible implications in pathogenesis of atherosclerosis, Biochim. Biophys. Acta - Lipids Lipid Metab. 1168 (1993) 115–121, http://dx.doi.org/10.1016/0005-2760(93)90274-D.

[61] A. Fredenrich, D. Jambou, P. Bayer, S. Hieronimus, P. Lapalus, M. Harter, Effects of low density and high density lipoproteins isolated from non-insulin dependent diabetic patients on prostaglandin secretion by mouse macrophage cell line P388D1, Atherosclerosis. 142 (n.d.), pp. 217–224. 〈http://dx.doi.org/10.1016/s0021-9150(98)00207-x〉.

[62] W. Fang, H. Li, L. Zhou, L. Su, Y. Liang, Y. Mu, Effect of prostaglandin E1 on TNF-induced vascular inflammation in human umbilical vein endothelial cells, Can. J. Physiol. Pharmacol. 88 (2010) 576–583, http://dx.doi.org/10.1139/y10-028.

[63] T.W. Faust, E. Lee, J.S. Redfern, M. Feldman, Effect of prostaglandin F3α on gastric mucosal injury by ethanol in rats: comparison with prostaglandin F2α,

Prostaglandins 37 (1989) 493–504, http://dx.doi.org/10.1016/0090-6980(89)90098-1.

[64] N.J. Spann, L.X. Garmire, J.G. McDonald, D.S. Myers, S.B. Milne, N. Shibata, D. Reichart, J.N. Fox, I. Shaked, D. Heudobler, C.R.H. Raetz, E.W. Wang, S.L. Kelly, M.C. Sullards, R.C. Murphy, A.H. Merrill Jr, H.A. Brown, E.A. Dennis, A.C. Li, K. Ley, S. Tsimikas, E. Fahy, S. Subramaniam, O. Quehenberger, D.W. Russell, C.K. Glass, Regulated accumulation of desmosterol integrates macrophage lipid metabolism and inflammatory responses, Cell 151 (2012) 138–152, http://dx.doi.org/10.1016/j.cell.2012.06.054.

[65] T. Simmet, B.A. Peskar, Prostaglandin, E 1 and arterial occlusive disease: pharmacological considerations, Eur. J. Clin. Invest. 18 (1988) 549–554, http://dx.doi.org/10.1111/j.1365-2362.1988.tb01266.x.

[66] J. Gdula-Argasińska, J. Czepiel, J. Totoń-Żurańska, P. Wołkow, T. Librowski, A. Czapkiewicz, W. Perucki, M. Woźniakiewicz, A. Woźniakiewicz, n-3 Fatty acids regulate the inflammatory-state related genes in the lung epithelial cells exposed to polycyclic aromatic hydrocarbons, Pharmacol. Rep. 68 (2016) 319–328, http://dx.doi.org/10.1016/j.pharep.2015.09.001.

[67] J.D. Brooks, E.S. Musiek, T.R. Koestner, J.N. Stankowski, J.R. Howard, E.M. Brunoldi, A. Porta, G. Zanoni, G. Vidari, J.D. Morrow, G.L. Milne, B. McLaughlin, The fatty acid oxidation product 15-A 3t-Isoprostane is a potent inhibitor of NFκB transcription and macrophage transformation, J. Neurochem. 119 (2011) 604–616, http://dx.doi.org/10.1111/j.1471-4159.2011.07422.x.